Filamentation in air with ultrashort mid-infrared pulses

Bonggu Shim,[1,2] **Samuel E. Schrauth,**[1] **and Alexander L. Gaeta**[1,3]

[1]*School of Applied and Engineering Physics, Cornell University,*
Ithaca, New York 14853, USA
[2]*bgs43@cornell.edu*
[3]*a.gaeta@cornell.edu*

Abstract: We theoretically investigate filamentation of ultrashort laser pulses in air in the mid-infrared regime under conditions in which the group-velocity dispersion (GVD) is anomalous. When a high-power, ultrashort mid-infrared laser beam centered at 3.1-μm forms a filament, a spatial solitary wave is stabilized by the plasma formation and propagates several times its diffraction length. Compared with temporal self-compression in gases due to plasma formation and pulse splitting in the normal-GVD regime, the minimum achievable pulse duration ($\sim$ 70 fs) is limited by the bandwidth of the anomalous-GVD region in air. For the relatively high powers, multiple pulse splitting due to the plasma effect and shock formation is observed, which is similar to that which occurs in solids. Our simulations show that the energy reservoir also plays a critical role for longer propagation of the air filament in the anomalous-GVD regime.

© 2011 Optical Society of America

OCIS codes: (010.1300) Atmospheric propagation; (320.7110) Ultrafast nonlinear optics.

References and links

1. A. Braun, G. Korn, X. Liu, D. Du, J. Squier, and G. Mourou,"Self-channeling of high-peak-power femtosecond laser pulses in air," Opt. Lett. **20**, 73–75 (1995), http://www.opticsinfobase.org/ol/abstract.cfm?URI=ol-20-1-73.
2. E. T. J. Nibbering, P. F. Curley, G. Grillon, B. S. Prade, M. A. Franco, F. Salin, and A. Mysyrowicz, "Conical emission from self-guided femtosecond pulses in air," Opt. Lett. **21**, 62–65 (1996), http://www.opticsinfobase.org/ol/abstract.cfm?URI=ol-21-1-62.
3. A. Brodeur, C. Y. Chien, F. A. Ilkov, S. L. Chin, O. G. Kosareva, and V. P. Kandidov, "Moving focus in the propagation of ultrashort laser pulses in air," Opt. Lett. **22**, 304–306 (1997), http://www.opticsinfobase.org/ol/abstract.cfm?URI=ol-22-5-304.
4. J. R. Peñano, P. Sprangle, B. Hafizi, A. Ting, D. F. Gordon, and C. A. Kapetanakos, "Propagation of ultra-short, intense laser pulses in air," Phys. Plasmas **11**, 2865 (2004).
5. A. Ting, I. Alexeev, D. Gordon, R. Fischer, D. Kaganovich, T. Jones, E. Briscoe, J. Peñano, R. Hubbard, and P. Sprangle, "Measurements of intense femtosecond laser pulse propagation in air," Phys. Plasmas **12**, 056705 (2005).
6. S. L. Chin, S. A. Hosseini, W. Liu, Q. Luo, F. Théberge, N. Aközbek, A. Becker, V. P. Kandidov, O. G. Kosareva, and H. Schroeder, "The propagation of powerful femtosecond laser pulses in opticalmedia: physics, applications, and new challenges," Can. J. Phys. **83**, 863–905 (2005).
7. A. Couairon and A. Mysyrowicz, "Femtosecond filamentation in transparent media," Phys. Rep. **441**, 47–189 (2007).
8. L. Bergé, S Skupin, R Nuter, J Kasparian, and J.-P. Wolf, "Ultrashort filaments of light in weakly ionized, optically transparent media," Rep. Prog. Phys. **70**, 1633 (2007).
9. J. Kasparian and J.-P. Wolf, "Physics and applications of atmospheric nonlinear optics and filamentation," Opt. Express **16**, 466–493 (2008), http://www.opticsinfobase.org/oe/abstract.cfm?URI=oe-16-1-466.

Report Documentation Page

1. REPORT DATE **04 APR 2011**	2. REPORT TYPE	3. DATES COVERED **00-00-2011 to 00-00-2011**

4. TITLE AND SUBTITLE **Filamentation in air with ultrashort mid-infrared pulses**	5a. CONTRACT NUMBER
	5b. GRANT NUMBER
	5c. PROGRAM ELEMENT NUMBER
6. AUTHOR(S)	5d. PROJECT NUMBER
	5e. TASK NUMBER
	5f. WORK UNIT NUMBER

7. PERFORMING ORGANIZATION NAME(S) AND ADDRESS(ES) **Cornell University ,School of Applied and Engineering Physics,ithaca,NY,14853**	8. PERFORMING ORGANIZATION REPORT NUMBER

9. SPONSORING/MONITORING AGENCY NAME(S) AND ADDRESS(ES)	10. SPONSOR/MONITOR'S ACRONYM(S)
	11. SPONSOR/MONITOR'S REPORT NUMBER(S)

12. DISTRIBUTION/AVAILABILITY STATEMENT
Approved for public release; distribution unlimited

13. SUPPLEMENTARY NOTES

14. ABSTRACT

We theoretically investigate filamentation of ultrashort laser pulses in air in the mid-infrared regime under conditions in which the group-velocity dispersion (GVD) is anomalous. When a high-power, ultrashort mid-infrared laser beam centered at 3.1-μm forms a filament, a spatial solitary wave is stabilized by the plasma formation and propagates several times its diffraction length. Compared with temporal self-compression in gases due to plasma formation and pulse splitting in the normal-GVD regime, the minimum achievable pulse duration ($\sim$ 70 fs) is limited by the bandwidth of the anomalous-GVD region in air. For the relatively high powers, multiple pulse splitting due to the plasma effect and shock formation is observed, which is similar to that which occurs in solids. Our simulations show that the energy reservoir also plays a critical role for longer propagation of the air filament in the anomalous-GVD regime.

15. SUBJECT TERMS

16. SECURITY CLASSIFICATION OF:			17. LIMITATION OF ABSTRACT	18. NUMBER OF PAGES	19a. NAME OF RESPONSIBLE PERSON
a. REPORT **unclassified**	b. ABSTRACT **unclassified**	c. THIS PAGE **unclassified**	**Same as Report (SAR)**	**9**	

10. V. P. Kandidov, S. A. Shlenov, and O. G. Kosareva, "Filamentation of high-power femtosecond laser radiation," Quantum Electron. **39**, 205 (2009).

11. L. Wöste, C. Wedekind, H. Wille, P. Rairoux, B. Stein, S. Nikolov, C. Werner, S. Niedermeier, F. Ronneberger, H. Schillinger, and R. Sauerbrey, "Femtosecond atmospheric lamp," Laser Optoelektron. **29**, 51 (1997).

12. P. Rairoux, H. Schillinger, S. Niedermeier, M. Rodriguez, F. Ronneberger, R. Sauerbrey, B. Stein, D. Waite, C. Wedekind, H. Wille, L. Wöste, and C. Ziener, "Remote sensing of the atmosphere using ultrashort laser pulses," Appl. Phys. B **71**, 573–580 (2000).

13. J.-C. Diels, R. Bernstein, K. Stahlkopf, and X. M. Zhao, "Lightning control with lasers," Sci. Am. **277**, 50–55 (1997).

14. R. P. Fischer, A. C. Ting, D. F. Gordon, R. F. Fernsler, D. P. DiComo, and P. Sprangle, "Conductivity measurements of femtosecond laserplasma filaments," IEEE Trans. Plasma Sci. **35**, 1430 (2007).

15. A. Houard, C. D'Amico, Y. Liu, Y. B. Andre, M. Franco, B. Prade, A. Mysyrowicz, E. Salmon, P. Pierlot, and L.-M. Cleon, "High current permanent discharges in air induced by femtosecond laser filamentation," Appl. Phys. Lett. **90**, 171501 (2007).

16. See, for example, *The Supercontinuum Laser Source*, ed. by R. R. Alfano (Springer-Verlag, 1989).

17. C. P. Hauri, W. Kornelis, F. W. Helbing, A. Heinrich, A. Couairon, A. Mysyrowicz, J. Biegert, and U. Keller, "Generation of intense, carrier-envelope phase-locked few-cycle laser pulses through filamentation," Appl. Phys. B **79**, 673–677 (2004).

18. C. D'Amico, A. Houard, M. Franco, B. Prade, A. Mysyrowicz, A. Couairon, and V. T. Tikhonchuk, "Conical forward THz emission from femtosecond-laser-beam filamentation in air," Phys. Rev. Lett. **98**, 235002 (2007).

19. K. D. Moll and A. L. Gaeta, "Role of dispersion in multiple-collapse dynamics," Opt. Lett. **29**, 995–997 (2004), http://www.opticsinfobase.org/ol/abstract.cfm?URI=ol-29-9-995.

20. A. Saliminia, S. L. Chin, and R. Vallée, "Ultra-broad and coherent white light generation in silica glass by focused femtosecond pulses at 1.5 um," Opt. Express **13**, 5731–5738 (2005), http://www.opticsinfobase.org/oe/abstract.cfm?URI=oe-13-15-5731.

21. M. A. Porras, A. Dubietis, A. Matijošius, R. Piskarskas, F. Bragheri, A. Averchi, and P. Di Trapani, "Characterization of conical emission of light filaments in media with anomalous dispersion," J. Opt. Soc. Am. B **24**, 581–584 (2007), http://www.opticsinfobase.org/josab/abstract.cfm?URI=josab-24-3-581.

22. M. Trippenbach and Y. B. Band, "Effects of self-steepening and self-frequency shifting on short-pulse splitting in dispersive nonlinear media," Phys. Rev. A **57**, 4791 (1998).

23. L. Bergé and S. Skupin, "Self-channeling of ultrashort laser pulses in materials with anomalous dispersion," Phys. Rev. E **71**, 065601 (2005).

24. J. Liu, R. Li, and Z. Xu, "Few-cycle spatiotemporal soliton wave excited with filamentation of a femtosecond laser pulse in materials with anomalous dispersion," Phys. Rev. A **74**, 043801 (2006).

25. L. Bergé and S. Skupin, "Few-cycle light bullets created by femtosecond filaments," Phys. Rev. Lett. **100**, 113902 (2008).

26. Although 3-D optical bullets are predicted to be unstable and have not been experimentally observed, several approaches have been theoretically proposed recently. For example, see [27–30].

27. M. Belić, N. Petrović, W.-P. Zhong, R.-H. Xie, and G. Chen, "Analytical light bullet solutions to the generalized (3+1)-dimensional nonlinear Schrödinger equation," Phys. Rev. Lett. **101**, 123904 (2008).

28. L. Torner and Y. V. Kartashov, "Light bullets in optical tandems," Opt. Lett. **34**, 1129–1131 (2009), http://www.opticsinfobase.org/ol/abstract.cfm?URI=ol-34-7-1129.

29. I. B. Burgess, M. Peccianti, G. Assanto, and R. Morandotti, "Accessible light bullets via synergetic nonlinearities," Phys. Rev. Lett. **102**, 203903 (2009).

30. S. Chen and J. M. Dudley, "Spatiotemporal nonlinear optical self-similarity in three dimensions," Phys. Rev. Lett. **102**, 233903 (2009).

31. I. G. Koprinkov, A. Suda, P. Wang, and K. Midorikawa, "Self-compression of high-intensity femtosecond optical pulses and spatiotemporal soliton generation," Phys. Rev. Lett. **84**, 3847–3850 (2000).

32. A. L. Gaeta and F. W. Wise, Comment on "Self-compression of high-intensity femtosecond optical pulses and spatiotemporal soliton generation," Phys. Rev. Lett. **87**, 229401 (2001).

33. L. Bergé and A. Couairon, "Gas-induced solitons," Phys. Rev. Lett. **86**, 1003–1006 (2001).

34. T.-T. Xi, X. Lu, and J. Zhang, "Interaction of light filaments generated by femtosecond laser pulses in air," Phys. Rev. Lett. **96**, 025003 (2006).

35. L. M. Kovachev, "Collapse arrest and self-guiding of femtosecond pulses," Opt. Express **15**, 10318–10323 (2007), http://www.opticsinfobase.org/oe/abstract.cfm?URI=oe-15-16-10318.

36. P. Agostini and L. F. DiMauro, "Atoms in high intensity mid-infrared pulses," Contemp. Phys. **49**, 179 (2008).

37. O. Chalus, A. Thai, P. K. Bates, and J. Biegert, "Six-cycle mid-infrared source with 3.8 μJ at 100 kHz," Opt. Lett. **35**, 3204–3206 (2010), http://www.opticsinfobase.org/ol/abstract.cfm?URI=ol-35-19-3204.

38. T. Popmintchev, M. Chen, P. Arpin, M. Gerrity, M. Seaberg, B. Zhang, D. Popmintchev, G. Andriukaitis, T. Balciunas, O. D. Mücke, A. Pugzlys, A. Baltuška, M. Murnane, and H. Kapteyn, "Bright coherent ultrafast X-rays from mid-IR lasers," in High Intensity Lasers and High Field Phenomena, OSA Technical Digest (CD)

(Optical Society of America, 2011), paper HThB5, `http://www.opticsinfobase.org/abstract.cfm?URI=HILAS-2011-HThB5`.

39. N. L. Wagner, E. A. Gibson, T. Popmintchev, I. P. Christov, M. M. Murnane, and H. C. Kapteyn, "Self-compression of ultrashort pulses through ionization-induced spatiotemporal reshaping," Phys. Rev. Lett. **93**, 173902 (2004).

40. A. Couairon, J. Biegert, C. P. Hauri, W. Kornelis, F. W. Helbing, U. Keller, and A. Mysyrowicz, "Self-compression of ultra-short laser pulses down to one optical cycle by filamentation," J. Mod. Opt. **53**, 75–85 (2006).

41. G. Stibenz, N. Zhavoronkov, and G. Steinmeyer, "Self-compression of millijoule pulses to 7.8 fs duration in a white-light filament," Opt. Lett. **31**, 274–276 (2006), `http://www.opticsinfobase.org/ol/abstract.cfm?URI=ol-31-2-274.`.

42. S. Skupin, G. Stibenz, L. Bergé, F. Lederer, T. Sokollik, M. Schnürer, N. Zhavoronkov, and G. Steinmeyer, "Self-compression by femtosecond pulse filamentation: Experiments versus numerical simulations," Phys. Rev. E **74**, 056604 (2006).

43. L. T. Vuong, R. B. Lopez-Martens, C. P. Hauri, and A. L. Gaeta, "Spectral reshaping and pulse compression via sequential filamentation in gases," Opt. Express **16**, 390–401 (2008), `http://www.opticsinfobase.org/oe/abstract.cfm?URI=oe-16-1-390`.

44. F. Reiter, U. Graf, E. E. Serebryannikov, W. Schweinberger, M. Fiess, M. Schultze, A. M. Azzeer, R. Kienberger, F. Krausz, A. M. Zheltikov, and E. Goulielmakis, "Route to attosecond nonlinear spectroscopy ," Phys. Rev. Lett. **105**, 243902 (2010).

45. T. Brabec and F. Krausz, "Nonlinear optical pulse propagation in the single-cycle regime," Phys. Rev. Lett. **78**, 3282–3285 (1997).

46. A. L. Gaeta, "Catastrophic collapse of ultrashort pulses," Phys. Rev. Lett. **84**, 3582–3585 (2000).

47. M. Kolesik, J. V. Moloney, and M. Mlejnek, "Unidirectional optical pulse propagation equation," Phys. Rev. Lett. **89**, 283902 (2002).

48. We calculate the dispersion parameters up to sixth-order order since the formula for the refractive index of air (n_0) is a function of the fifth-order Taylor expansion in Ref. [49] and thus the wavelumber ($k = \omega n_0/c$) is a sixth-order function of the laser angular frequency.

49. R. J. Mathar, "Refractive index of humid air in the infrared: model fits," J. Opt. A, Pure Appl. Opt. **9**, 470 (2007).

50. R. J. Mathar, "Calculated refractivity of water vapor and moist air in the atmospheric window at 10 μm," Appl. Opt. **43**, 928 (2004).

51. See, for example, `http://irina.eas.gatech.edu/irina/eas8803_fall2009/Lec6.pdf`.

52. G. Fibich and A. L. Gaeta, "On the critical power for self-focusing in bulk media and in hollow waveguides," Opt. Lett. **25**, 335–337 (2000), `http://www.opticsinfobase.org/ol/abstract.cfm?URI=ol-25-5-335`.

53. J. Lehmeier, W. Leupacher, and A. Penzkofer, "Nonresonant third order hyperpolarizability of rare gases and N_2 determined by third harmonic generation," Opt. Commun. **56**, 67–72 (1985).

54. A. A. Zozulya, S. A. Diddams, and T. S. Clement, "Investigations of nonlinear femtosecond pulse propagation with the inclusion of Raman, shock, and third-order phase effects," Phys. Rev. A **58**, 3303–3310 (1998).

55. G. P. Agrawal, *Nolinear Fiber Optics*, (Academic Press, 2007).

56. M. Mlejnek, M. Kolesik, J. V. Moloney, and E. M. Wright, "Optically turbulent femtosecond light guide in air," Phys. Rev. Lett. **83**, 2938–2941 (1999).

57. M. Kolesik and J. V. Moloney, "Self-healing femtosecond light filaments," Opt. Lett. **29**, 590–592 (2004), `http://www.opticsinfobase.org/ol/abstract.cfm?URI=ol-29-6-590`.

58. F. Courvoisier, V. Boutou, J. Kasparian, E. Salmon, G. Méjean, J. Yu, and J.-P. Wolf, "Ultraintense light filaments transmitted through clouds," Appl. Rev. Lett. **83**, 213 (2003).

59. A. Dubietis, E. Gaižauskas, G. Tamošauskas, and P. Di Trapani, "Light filaments without self-channeling," Phys. Rev. Lett. **92**, 253903 (2004).

60. G. Méchain, G. Méjean, R. Ackermann, P. Rohwetter, Y.-B. André, J. Kasparian, B. Prade, K. Stelmaszczyk, J. Yu, E. Salmon, W. Winn, L. A. (Vern) Schlie, A. Mysyrowicz, R. Sauerbrey, L. Wöste, and J.-P. Wolf, "Propagation of fs TW laser filaments in adverse atmospheric conditions," Appl. Phys. B **80**, 785–789 (2005).

61. W. Liu, F. Théberge, E. Arévalo, J.-F. Gravel, A. Becker, and S. L. Chin, "Experiment and simulations on the energy reservoir effect in femtosecond light filaments," Opt. Lett. **30**, 2602–2604 (2005), `http://www.opticsinfobase.org/ol/abstract.cfm?URI=ol-30-19-2602`.

62. S. Eisenmann, J. Peñano, P. Sprangle, and A. Zigler, "Effect of an energy reservoir on the atmospheric propagation of laser-plasma filaments," Phys. Rev. Lett. **100**, 155003 (2008).

63. Z. Hao, J. Zhang, X. Lu, T. Xi, Z. Zhang, and Z. Wang, "Energy interchange between large-scale free propagating filaments and its background reservoir," J. Opt. Soc. Am. B **26**, 499–502 (2009), `http://www.opticsinfobase.org/josab/abstract.cfm?URI=josab-26-3-499`.

1. Introduction

Self-channeling beams (*i.e.* filaments) in air with high-power, ultrashort pulses have been shown to propagate several diffraction lengths with little apparent change in the beam shape due to the balance between self-focusing and diffraction/plasma formation [1–10]. These filaments have received significant attention due to applications to remote sensing [11, 12], lightning guiding [13–15], supercontinuum generation (SCG) [16], pulse compression [17], and THz generation [18]. Although several experimental [19–21] and theoretical studies in solids [22–25] for filamentation and soliton generation in the anomalous group-velocity dispersion (GVD) regime have been reported recently [26–30], studies of air (or gas) filaments have been limited to the normal-GVD regime [25, 31–35]. Only recently has the ability of laser technology with difference-frequency generation (DFG) [36] and optical parametric chirped-pulse amplification (OPCPA) [37, 38] been developed to produce > 100-GW pulses in the mid-infrared region where the GVD is anomalous, and investigations of self-focusing in air in the anomalous-GVD regime are now a possibility.

In this Letter, we present the first simulation results for air filamentation and spatial solitary-wave formation in the anomalous-GVD regime of air. When a high-power (> 100-GW), ultrashort pulse undergoes self-focusing due to the Kerr nonlinearity, multi-photon absorption (MPA) and plasma formation halt beam collapse. As a result, a spatial solitary wave is formed and stabilized during the filamentation process, and its shape can be maintained for several diffraction lengths. Although spectral broadening induced by phase modulation occurs, the relatively narrow bandwidth of the anomalous-GVD regime (approximately 200-nm) near 3-μm inhibits formation of a temporal solitary wave, which contrasts to the generation of few-cycle optical pulses predicted for solids in the broadband anomalous-GVD region [23, 24] and to pulse self-compression down to few-cycles which occurs via plasma formation and/or pulse splitting in gases for the normal-GVD regime [31, 32, 39–44].

2. Simulation and refractive index of air

In our simulations, we use the radially-symmetric nonlinear envelope equation (NEE) in normalized units including diffraction, dispersion, self-focusing with the delayed Raman response, MPA, and plasma de-focusing and absorption, which is given as [23, 43, 45–47],

$$
\begin{aligned}
\frac{\partial \psi}{\partial \zeta} &= \frac{i}{4}\left(1+\frac{i\partial}{\omega\tau_p\partial\tau}\right)^{-1}\nabla_\perp^2\psi + iL_{df}\sum_{n=2}^{n=6}\frac{\beta_n}{n!}\left(\frac{i\partial}{\tau_p\partial\tau}\right)^n\psi \\
&+ i\left(1+\frac{i\partial}{\omega\tau_p\partial\tau}\right)\frac{L_{df}}{L_{nl}}\left(\frac{|\psi|^2}{2}+\frac{\tau_p}{2\tau_k}\int_{-\infty}^{\tau}e^{-\frac{\tau_p}{\tau_k}(\tau-\tau')}|\psi(\tau')|^2 d\tau'\right)\psi \\
&- \frac{L_{df}}{2L_{mp}}\frac{\psi}{|\psi|^2}\frac{\partial\eta}{\partial\tau} - \frac{L_{df}}{L_{pl}}\left(i+\frac{1}{\omega\tau_c}\right)\eta\left(\psi+\frac{\frac{\tau_c\partial\psi}{\tau_p\partial\tau}}{1-i\omega\tau_c}\right),
\end{aligned}
\tag{1}
$$

where ψ is the field normalized by the peak input field amplitude A_0, $\zeta = z/L_{df}$ is the propagation distance normalized by the diffraction length $L_{df} = n_0\pi w_0^2/\lambda_0$, n_0 is the refractive index of air, w_0 is the $1/e^2$ spot size radius, λ_0 is the central wavelength, $\nabla_\perp^2$ is the transverse Laplacian, τ is the retarded time normalized by the $1/e^2$ input pulse duration τ_p, β_n is the nth-order dispersion parameter [48], $L_{nl} = c/(\omega n_2 I_0)$ is the nonlinear length, n_2 is the nonlinear refractive index, $I_0 = cn_0|A_0|^2/2\pi$ is the peak input intensity, $\tau_k = 70$ fs is the Raman relaxation time, $L_{mp} = 1/(\beta^{(m)}I_0^{(m-1)})$ is the m-photon absorption length, $\beta^{(m=31)} = 3\times10^{-384}$ cm^{59}/W^{30} is the 31-photon absorption coefficient [7], $L_{pl} = 2/(\sigma\rho_0\omega\tau_c)$ is the plasma length, σ is the inverse bremsstrahlung cross section, $\rho_0 = \beta^{(m)}I_0^{(m-1)}\tau_p/(m\hbar\omega)$ is the total electron density that would

be produced by the input laser pulse via multi-photon ionization, τ_c is the electron-ion collision time, $\eta = \rho_e/\rho_0$ is the normalized electron density. The operator $(1 + i\partial/\omega\tau_p\partial\tau)$ accounts for space-time focusing in the diffraction term and self-steepening in the self-focusing term. The plasma is generated by multi-photon ionization and avalanche ionization, and the electron density satisfies the equation,

$$\frac{\partial \eta}{\partial \tau} = |\psi|^{2m} + \alpha\eta|\psi|^2, \qquad (2)$$

where $\alpha = \sigma I_0 \tau_p/(n_0^2 E_g)$ is the avalanche ionization coefficient, and E_g = 12.1 eV the band-gap energy for oxygen.
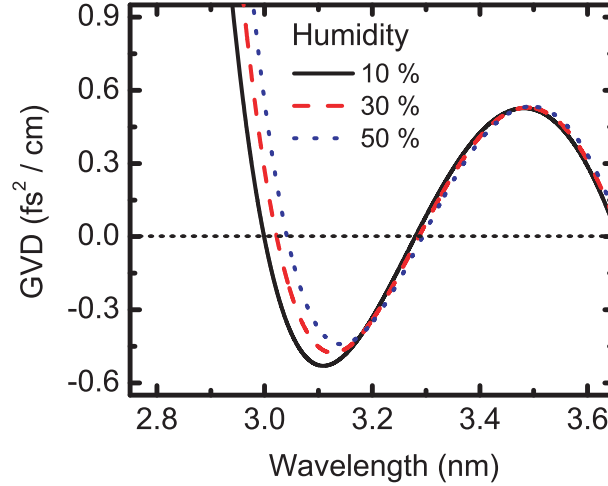

Fig. 1. Calculated group-velocity dispersion (GVD) for different values of the humidity using the Taylor expansion formula based on Ref. [49] at T = 17.5°C, p = 101325 Pa (standard atmospheric pressure).

The dispersion parameters at 3.1-μm are calculated using the Taylor expansion formula, which is a function of wavelength λ, temperature T, pressure p, and humidity h [49]. Figure 1 shows the calculated GVD for different values of humidity at T = 17.5°C and p = 101,325 Pa (standard atmospheric pressure). As humidity and temperature (not shown) increase, the absolute magnitude of the GVD and the wavelength range of anomalous GVD decrease slightly, and the peak of the GVD shifts toward longer wavelengths. We assume 10 % humidity ($h = 10$) for our calculations such that β_2 = -0.53 fs^2/cm, β_3 = 3.02 fs^3/cm, and higher-order dispersion parameters ($n \geq 4$) are all positive. The anomalous-GVD region near 3.1-μm which spans 200-nm is related to the water vapor absorption, and the fitting coefficients used for index calculation are valid between 2.8-μm and 4.2-μm. There exist strong resonance absorption regions between $2.5 - 2.8$-μm and $4.2 - 4.4$-μm due to the presence of water vapor and carbon dioxide (CO_2) [49–51]. The calculated critical power $P_{cr} = \alpha\lambda^2/(4\pi n_0 n_2)$, where $\alpha = 1.8962$ for the input Gaussian beam profile [52], is equal to 66-GW [53]. We limit the peak power of the input pulse $P \leq 8P_{cr}$ to avoid multi-filamentation.

3. Results and discussion

Figure 2(a) shows a plot of the peak intensity as a function of normalized distance for different input powers. Here we assume the collimated, initial spot size (1/e^2 radius) is 12-mm and the initial pulse duration (FWHM) is 150 fs such that L_{df} = 146-m approximately matches
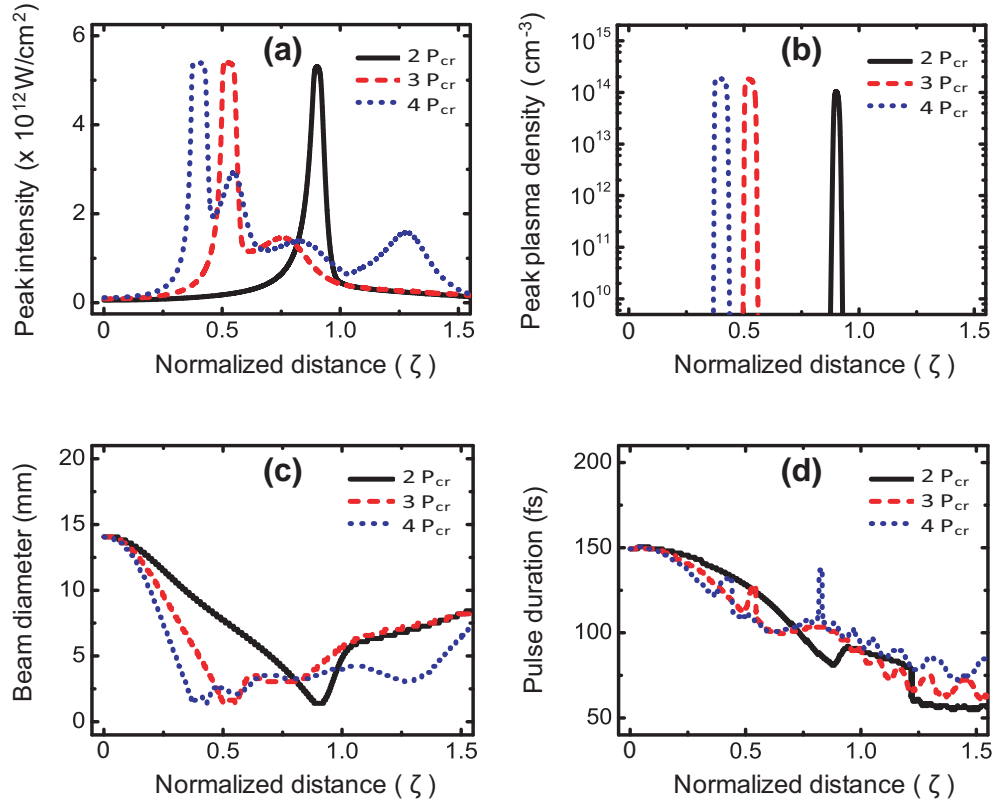
Fig. 2. Calculated (a) peak intensity, (b) peak plasma density, (c) beam diameter (FWHM) of the fluence $F_r = \int I(r,t)dt$ and (d) pulse duration (FWHM) of the fluence $F_t = \int I(r,t)rdr$ as functions of normalized propagation distance for various input powers.

with $L_{ds} = \tau_p^2/\beta_2 = 306$-m. As the peak intensity increases due to self-focusing and anomalous GVD, a low-density plasma is created as shown in Fig. 2(b). At that point, plasma absorption and de-focusing combined with MPA arrest beam collapse so that an air filament with $I = 5 \times 10^{12}$ W/cm^2 forms and propagates stably about 0.03, 0.05 and 0.06 times the diffraction length of the input beam for $P/P_{cr} = 2$, 3 and 4. For increasing powers, collapse occurs at shorter distances, and the filament length is extended. According to the calculated beam diameter (FWHM) [Figs. 2(c)], the filament maintains its diameter (1.4-mm FWHM), which is 1/10 that of the initial beam and thus a spatial solitary wave is generated during filamentation, propagating for at least 3 times of the diffraction length based on its minimum spot size. As is shown in Fig. 2(d), although the pulse duration initially decreases due to anomalous GVD, it suddenly increases near the peak intensity due to spectral broadening into the normal GVD regime via self-phase modulation and slowly decreases again since the field components at wavelengths in the anomalous GVD regime undergo compression as the pulse propagates. Therefore, compared with calculated few-cycle spatio-temporal solitary waves in the anomalous-GVD regime for solids [23, 24], a solitary wave is not generated near 3.1-μm due to the relatively narrow bandwidth of the anomalous-GVD region.

Figure 3(a) shows examples of the spatio-temporal intensity distributions for various propagation distances with $P/P_{cr} = 2$. As the beam self-focuses, self-steepening and space-time focusing combined with third-order dispersion generate a relatively steep edge at the rear of
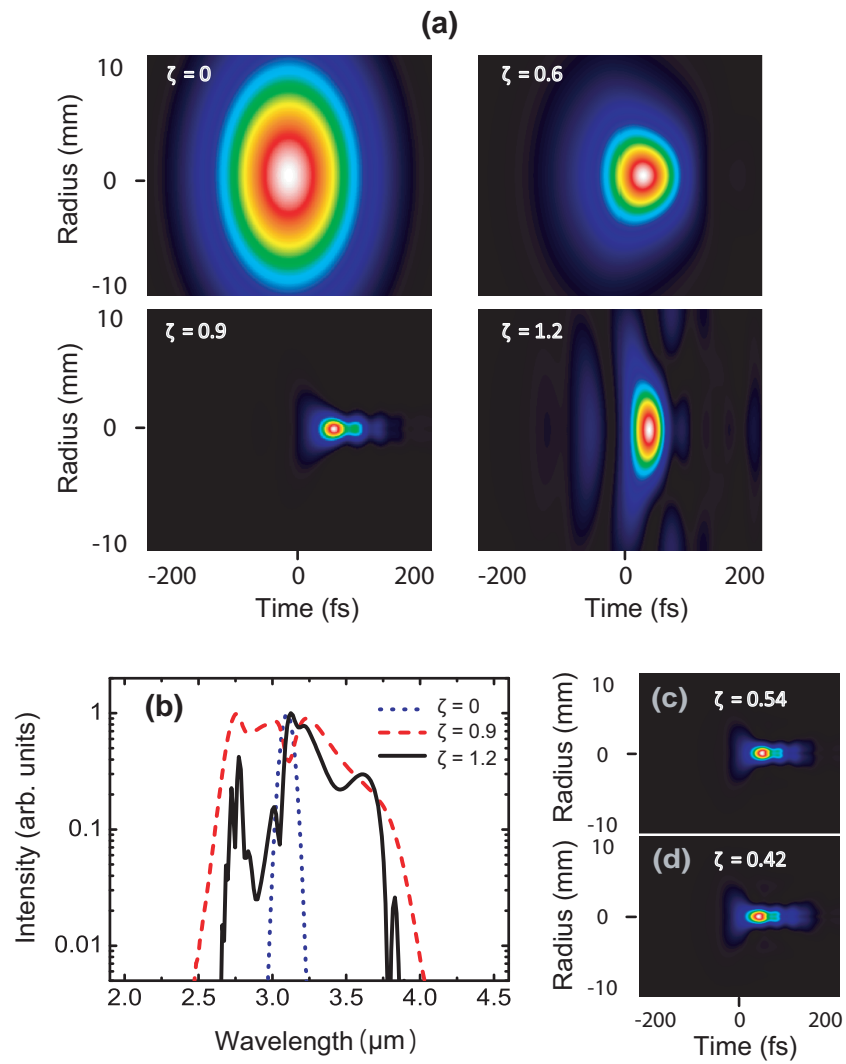
(a)

Fig. 3. (a) Spatio-temporal intensity profiles at various propagation distances $\zeta = z/L_{df}$ for $P/P_{cr} = 2$. (b) On-axis spectra at various propagation distances for $P/P_{cr} = 2$. (c) Spatiotemporal intensity profiles of collapsing pulses at $\zeta = 0.54$ for $P/P_{cr} = 3$, and (d) at $\zeta = 0.42$ for $P/P_{cr} = 4$

the pulse (*i.e.*, an optical shock) and push the pulse toward positive times [23, 24, 46, 54, 55] [see Fig. 3(a) at $\zeta = 0.6$]. Subsequently, the pulse collapses at $\zeta = 0.9$, and SCG occurs as shown in the on-axis spectra [Fig. 3(b)]. Blue-shifted wavelength components in the normal-GVD regime (*i.e.*, below 3-μm in Fig. 1) that are generated by the optical shock form a long trailing edge [24], and it diffracts as the beam loses its energy by MPA and plasma generation. Similar spatio-temporal behavior during beam collapse and filament generation is observed for $P/P_{cr} = 3$ and 4 [Figs. 3(c) and 3(d)].
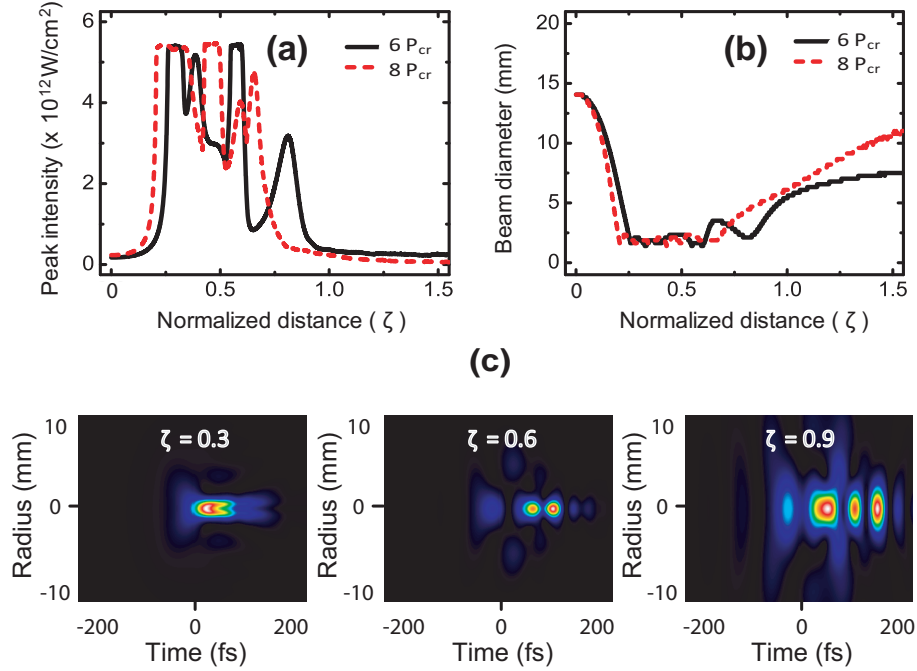

Fig. 4. Calculated (a) peak intensity, (b) beam diameter (FWHM) as functions of normalized propagation distance for $P/P_{cr} = 6$ and 8. (c) Examples of spatio-temporal intensity profiles at various distances for $P/P_{cr} = 6$.

Multiple collapse is observed for higher powers ($P/P_{cr} = 6$ and 8), as experimentally demonstrated in solids [19] [Fig. 4(a)]. Although similar spatio-temporal shapes are generated in the first collapse region, as in the case at low powers, plasma defocusing and refocusing in the temporal domain combined with strong shock terms produce pulse-splitting accompanied by complicated temporal dynamics such as further splitting and energy transfer between split pulses in the secondary collapse regions [Fig. 4(c)] [23].

The role of the background energy reservoir supplying the energy into the filament core which contains approximately one critical power when it loses energy due to mechanisms such as MPA has been studied by many groups [56–63]. We also compare air-filament propagation for $P/P_{cr} = 6$ by simulating the placement of apertures with different diameters that block a fraction of the reservoir energy [Fig. 5]. Simulation results show that the filament length and the number of multiple collapse regions decrease with apertures, which confirms that the background energy is important for longer propagation of the filamen, as is the case in the normal-GVD regime.
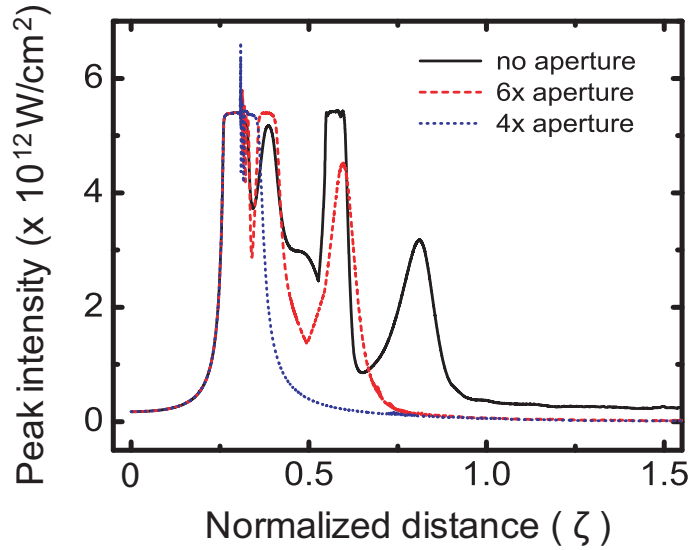
Fig. 5. Air filament formation and propagation with apertures of which sizes are 4 and 6 times of the minimum spot size ($\sim$ 1.2-mm) at $\zeta = 0.3$ for $P/P_{cr} = 6$.

4. Conclusion

In conclusion, we investigate air filamentation for relatively large diameters in the anomalous-GVD regime centered at 3.1-μm. The mm-sized filament can propagate several times its diffraction length, and the propagation distance increases with the higher laser input power. However, the potential formation of a spatio-temporal solitary wave is inhibited by the narrow bandwidth of the anomalous-GVD regime. Two other wavelength regions below 10-μm with the anomalous-GVD and weak absorption include two 100-nm bandwidth regions centered at 4.7 μm related to CO_2 absorption and at 9.5 μm related to O_3 absorption [49–51]. Since the high-power, ultrashort mid-infrared laser technology has rapidly progressed in recent years, we expect that the necessary power ($>$ 100-GW) for experimental studies should be available soon [36–38].

Acknowledgments